inter.noise
21-24 AUGUST
SCOTTISH EVENT CAMPUS
GLASGOW 2022

The effects of different types of noise on thermoacoustic systems using a Green's function approach

Sadaf Arabi[1]
Keele University
School of Physical and Chemical Sciences, Keele University, Staffordshire ST5 5BG, United Kingdom

Maria Heckl[2]
Keele University
School of Physical and Chemical Sciences, Keele University, Staffordshire ST5 5BG, United Kingdom

ABSTRACT

In this paper, we take advantage of using a Green's function approach as an analytical tool to study linear and nonlinear aspects of thermoacoustic systems. Green's function is defined as the impulse response of a system; it has a clear physical meaning in combustion systems, and it provides a fast and flexible tool to predict thermoacoustic instabilities in both time and frequency domains. In this study, we consider a tube, which houses two sources: a heat source and an external noise source. The heat source is modelled by an amplitude-dependent $n\tau$-law, the noise source is assumed to emit two types of noise (pink noise or white noise). We use the Green's function approach to derive an integral equation for the acoustic field in the Rijke tube, and we also derive an algebraic equation for the thermoacoustic eigenfrequency. Both equations are validated. The results that we found, show that the presence of noise (whether pink or white noise) results in "triggering" an instability and in accelerating the growth of the amplitude. These effects become more pronounced as the level of noise increases. The influence of pink noise is stronger than that of white noise. We also studied how the hysteresis behavior (a nonlinear effect in dynamical systems) is affected by the noise, using the heater power as bifurcation parameter. Our study reveals that the width of the bistable region decreases as the strength of noise increases.

1. INTRODUCTION

Development of new combustion systems to reduce the pollutants and increase the performance of combustion systems motivated scientists to study combustion instabilities in detail. Thermoacoustic instabilities occur due to the feedback mechanism between the flame and acoustic waves within the combustion chamber. The importance of predicting the thermoacoustic instabilities based on an analytical method led to applying a Green's function approach to thermoaocustic systems in both time and frequency domains [1][2][3]. Using a Green's function approach and combining it with Lighthill's acoustic analogy equation with a nonlinear forcing term in [3] exhibited the capability of this method to capture limit cycle amplitudes and hysteresis effects.

[1] s.arabi@keele.ac.uk.com

[2] m.a.heckl@keele.ac.uk

Combustion systems are inherently noisy. This motivated many investigations to include different types of the noise in the system [4][5]. The nonlinear dynamical behaviors (e.g., limit cycle, triggering and hysteresis effects) of such systems have been observed in experimental and analytical methods. [6][7]

In order to assess the capability of a Green's function approach to explore different phenomena in the presence of noise, we considered two types of noise (white and pink noise), coming from an external source. In section 2, we describe the mathematical model using our Green's function approach. In section 3, the flame model and noise model will be presented. In section 4, the governing equation is given to predict thermoacoustic instabilities. Finally, section 5 will present some results in the presence of noise.

2. The tailored Green's function

The tailored Green's function is determined as an impulsive response of the system with point source at (x', t') observed at (x, t) with defined boundaries Equation (1). It is assumed that Green's function can be written as superposition of modes Equation (2) for a tube shown in Figure 1. $H(t-t')$ denotes the Heaviside function; g_n is modal amplitude and ω_n is modal frequency in Green's function.

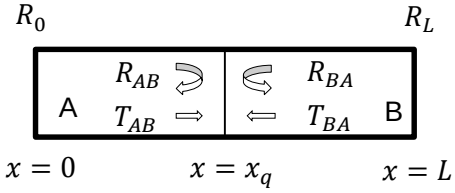

Figure 1: Tube of length L with inlet and outlet reflection coefficients (R_0, R_L) and an interface with temperature jump within the tube at x_q that divides the tube into regions A and B. The reflection and transmission coefficients for the interface are R_{AB}, T_{AB}, R_{BA} and T_{BA}.

The temperature, density and the speed of sound in the cold region (A) are $\bar{T}_1, \bar{\rho}_1, c_1$, and in the hot region (B), they are $\bar{T}_2, \bar{\rho}_2, c_2$, respectively.

$$\frac{1}{c^2}\frac{\partial^2 G}{\partial t^2} - \frac{\partial^2 G}{\partial x^2} = \delta(x-x')\delta(t-t') \tag{1}$$

$$G(x, x', t, t') = H(t-t')\, Re \sum_{n=1}^{\infty} g_n(x, x') e^{-i\omega_n (t-t')} \tag{2}$$

In order to obtain the modal frequencies and amplitudes in Equation (2), we use the equations derived by [2]; these are given below in Equations (3) and (4). The characteristic equation (Equation (3)) can be solved with a numerical root finding method (e.g., Newton Raphson method).

$$\begin{aligned} F(\omega) = {} & e^{-ik_1 x_q}\, e^{ik_2 (x_q - L)} - R_{BA} R_L\, e^{-ik_1 x_q}\, e^{-ik_2 (x_q - L)} - R_0 R_{AB} e^{ik_1 x_q}\, e^{ik_2 (x_q - L)} \\ & + R_0 R_L\, e^{ik_1 x_q}\, e^{-ik_2 (x_q - L)} \left(R_{AB} R_{BA} - T_{AB} T_{BA}\right) \end{aligned} \tag{3}$$

The modal amplitudes are calculated from Equation (4),

$$g_n(x,x') = \frac{c_2 \hat{g}(x,x',\omega)}{\omega_n F'(\omega_n)} \tag{4}$$

where

$$\hat{g} = \begin{cases} A(x,\omega)\, B(x',\omega) & 0 < x < x_q \\ B(x',\omega)\, C(x,\omega) & x_q < x < x' \\ C(x',\omega)\, B(x,\omega) & x' < x < L \end{cases} \tag{5}$$

$$A(x,\omega) = T_{BA}\left(R_0\, e^{ik_1 x} + e^{-ik_1 x}\right) \tag{6}$$

$$B(x,\omega) = e^{ik_2(x-L)} + R_L\, e^{-ik_2(x-L)} \tag{7}$$

$$C(x,\omega) = e^{ik_2(x-x_q)}\left(R_{BA} e^{-ik_1 x_q} + R_0\, e^{ik_1 x_q}\right) + e^{-ik_2(x-x_q)}\left(e^{-ik_1 x_q} - R_{AB} R_0 e^{ik_1 x_q}\right) \tag{8}$$

3. Heat release rate and noise models

In this paper, the heat release rate is modelled by a generalized nτ-law model, given in Equation (9). K is the heater power, and it is given in Equation (10). The terms n_0, n_1 and τ depend on the amplitude A of the acoustic field in the tube, as shown in Equations (11)-(14). We assume that the heat source is a point source at position (x_q), and describe it by $q(t,x) = q(t)\delta(x - x_q)$,

$$q(t) = K\left[n_1 u_q(t-\tau) - n_0 u_q(t)\right] \tag{9}$$

$$K = \frac{\bar{Q}}{\bar{U} s \bar{\rho}} \tag{10}$$

$$n_1 = \frac{g_{max}(A) + 1}{2} \tag{11}$$

$$n_0 = \frac{g_{max}(A) - 1}{2} \tag{12}$$

$$g_{max} = g_0 - g_1\left(\frac{A}{\bar{U}}\right) \tag{13}$$

$$\tau = \tau_0 + \tau_2\left(\frac{A}{\bar{U}}\right)^2 \tag{14}$$

The noise is considered as an external acoustic source, also concentrated at the point x_q. We describe it by a forcing term, which is added to the heat source term in Lighthill's acoustic analogy equation. Two types of noise will be considered: white and pink noise. The main difference between these two noise types is in the frequency spectrum of the power density: in white noise, the power density does not change with frequency, whereas in pink noise it decreases significantly as the frequency increases. It has been established that the features of colored noise are a better representation for the noisy environment found in combustion systems [8].

4. Derivation of integral governing equation in presence of the noise

The derivation of the integral governing equation in the absence of noise has been described in detail in [3]. If noise is present, a forcing term due to noise enters the picture (see Equation (15), where $F_n(x,t)$ denotes the noise term).

$$\frac{1}{c^2}\frac{\partial^2\phi}{\partial t^2} - \frac{\partial^2\phi}{\partial x^2} = -\frac{\gamma-1}{c^2}\,q(x,t) + F_n(x,t) \tag{15}$$

The initial conditions for our system are set as

$$\phi(x,0) = \varphi_0\,\delta(x-x_q) \qquad \frac{\partial\phi(x,0)}{\partial t} = \varphi_0'\,\delta(x-x_q) \tag{16}$$

By combining Equation (15) and Equation (2), we obtain the integral governing equation given in Equation (17). In order to find the time evolution of the thermoacoustic system, we use Equation (17) and solve it numerically with an iteration in time. This gives the time history of the acoustic field (see [3]). We consider noise term as a point source at the flame position, so $F_n(x,t) = F_n(t)\delta(x-x_q)$

$$\begin{aligned} u_q(t) = \left.\frac{\partial\phi}{\partial x}\right|_{x=x_q} &= -\frac{\gamma-1}{c^2}\int_{t'=0}^{t}\left.\frac{\partial G(x,x',t,t')}{\partial x}\right|_{\substack{x=x_q\\x'=x_q}} q(t')\,dt' \\ &+ \int_{t'=0}^{t}\left.\frac{\partial G(x,x',t,t')}{\partial x}\right|_{\substack{x=x_q\\x'=x_q}} F_n(t')\,dt' - \frac{\varphi_0}{c^2}\left.\frac{\partial G}{\partial x\partial t'}\right|_{\substack{x=x_q\\x'=x_q\\t'=0}} + \frac{\varphi_0'}{c^2}\left.\frac{\partial G}{\partial x}\right|_{\substack{x=x_q\\x'=x_q\\t'=0}} \end{aligned} \tag{17}$$

One of the advantages of using a Green's function approach for thermoacoustic systems is its capability to give results not only in the time domain, but also in the frequency domain. In order to perform a frequency-domain analysis, we write the acoustic field as superposition of heat-driven modes with frequencies Ω_m and velocity amplitudes u_m; this is shown in Equation (18).

$$u_q(t) = \sum_{m=1}^{\infty}\left(u_m e^{-i\Omega_m t} + u_m^* e^{i\Omega_m^* t}\right) \tag{18}$$

$\Omega_m$is complex; its real part gives the heat driven frequencies, and its imaginary part gives the growth rates. By using the Equation (18) and substituting it into the integral governing equation (17), we find a set of equations (Equations (19) and (20)) that provides the information about heat driven frequencies and growth rates. In addition, we can find the heat driven velocity amplitudes. (For more details, see [3])

$$\left(n_1 e^{i\Omega_m \tau} - n_0\right)\left(\frac{G_n}{i(\omega_n - \Omega_m)} + \frac{G_n^*}{i(-\omega_n^* - \Omega_m)}\right) = -\frac{2c^2}{K(\gamma - 1)} \tag{19}$$

$$\frac{u_m\left(n_1 e^{i\Omega_m \tau} - n_0\right)}{i(\omega_n - \Omega_m)} + \frac{u_m^*\left(n_1 e^{-i\Omega_m^* \tau} - n_0\right)}{i(\omega_n + \Omega_m^*)} = \frac{F_n\left(e^{i\omega_n t} - 1\right)}{i\omega_n} \times \frac{c^2}{K(\gamma - 1)} + \frac{i\omega_n \varphi_0 + \varphi_0'}{K(\gamma - 1)} \tag{20}$$

5. Results

In order to validate the time and frequency domain approaches using Green's function to find the acoustic field, we performed a comparison between these two different approaches. To have an insight about the stability behavior of a thermoacoustic system, we can use Equation (19) to produce a stability map. Hence, we consider a Rijke tube $(R_0 = -1, R_L = -1)$, that its length is $L = 2$. The temperature in the cold and hot regions are $\overline{T}_A = 304\ K$ and $\overline{T}_B = 460\ K$, respectively. The values of the heat release rate parameters are set as $\tau_0 = 5 \times 10^{-3} s, \tau_2 = 4.4 \times 10^{-3} s, g_0 = 1.4, g_1 = 0.3$. Figure 2 exhibited the stability map for Rijke tube for different values of heat source position. The black regions show the unstable region and white ones are related to stable regions.

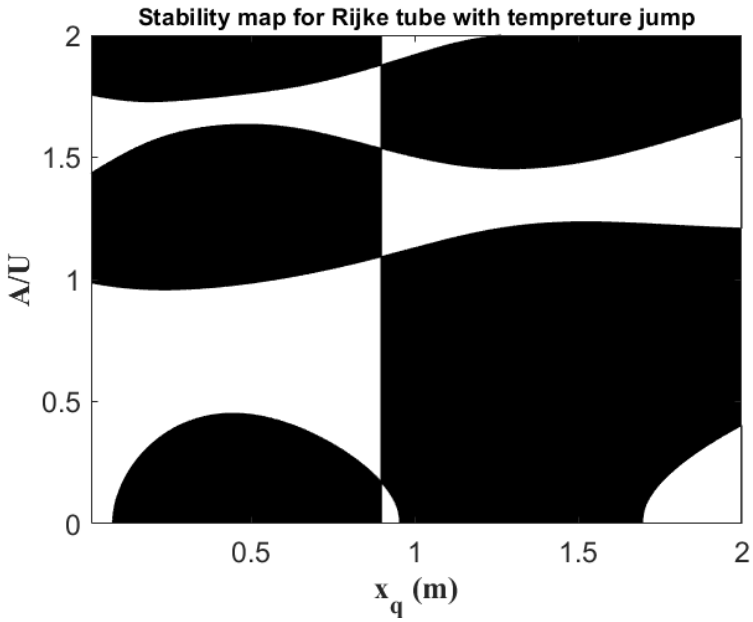

Figure 2: Stability map for Rijke tube with temperature jump, black regions are unstable and white regions are stable.

We selected a specific point $(x_q = 0.4, \frac{A}{U} = 0.01)$ in the upstream part of the Rijke tube. As Figure 3a indicates, the behavior of this point is unstable, and we observe a growth in amplitude, leading to a limit cycle. This Figure 3a has been calculated by solving Equation (17) with an iteration stepping forward in time. It should be noted that this time history is for the noiseless case, i.e. the

noise term is zero ($F_n(t) = 0$). In order to prove our assumption in section 4 that the acoustic field can be written as in Equation (18), we need to find the complex heat-driven frequencies Ω_m and heat-driven amplitudes u_m for the noiseless case (see Equations (19) and (20)). For this purpose, we chose two time intervals: one during the transient stage and the other one during the limit cycle stage. As Figure 3b and Figure 3c show, there is good agreement of the results from the time-domain calculation with those from the frequency-domain calculation. We conclude that both calculations provide reliable predictions of the behavior of the thermoacoustic system.

a)

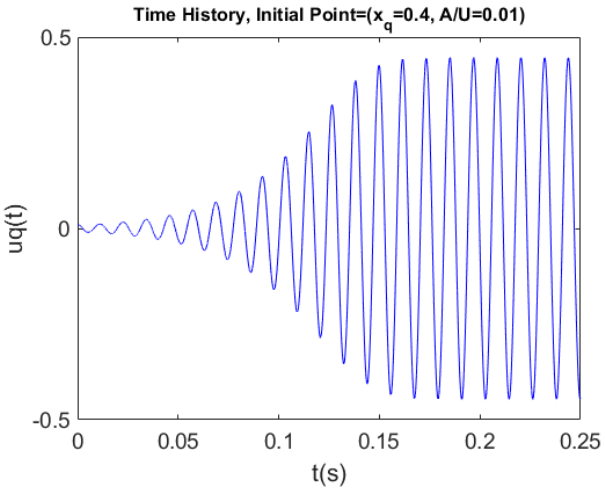

b)

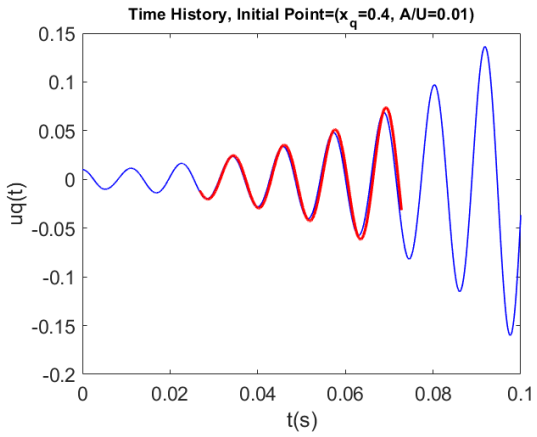

c)

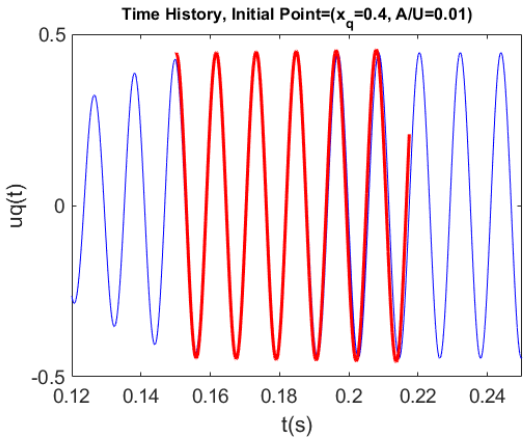

Figure 3: a) Time evolution in noiseless case using the time domain data. b) Comparison the results for the acoustic field in the time domain (blue curve) and frequency domain (red curve) during the transient stage c) Comparison of the results for the acoustic field in the time domain (blue curve) and frequency domain (red curve) during the limit cycle stage

The effect of noise on the time history of a thermoacoustic system has been reported in [9]. Now, we compare the effects of the white and pink noise on the stability behavior of the system. Figure 4 shows the time history for a point in the downstream part of a Rijke tube. The behavior of system in the noiseless case (blue curve) is stable, since we have a decay in amplitude to reach to zero. In each step, we added white and pink noise to our system. As we increase the level of noise (β) in Figure 4a, Figure 4b and Figure 4c the behavior of system does not change, but when $\beta = 6$ the pink noise triggers the instability and makes the system unstable. However, for the white noise, it is

still stable. Basically, the presence of noise can trigger a thermoacoustic instability. The pink noise is a more effective trigger than the white noise.

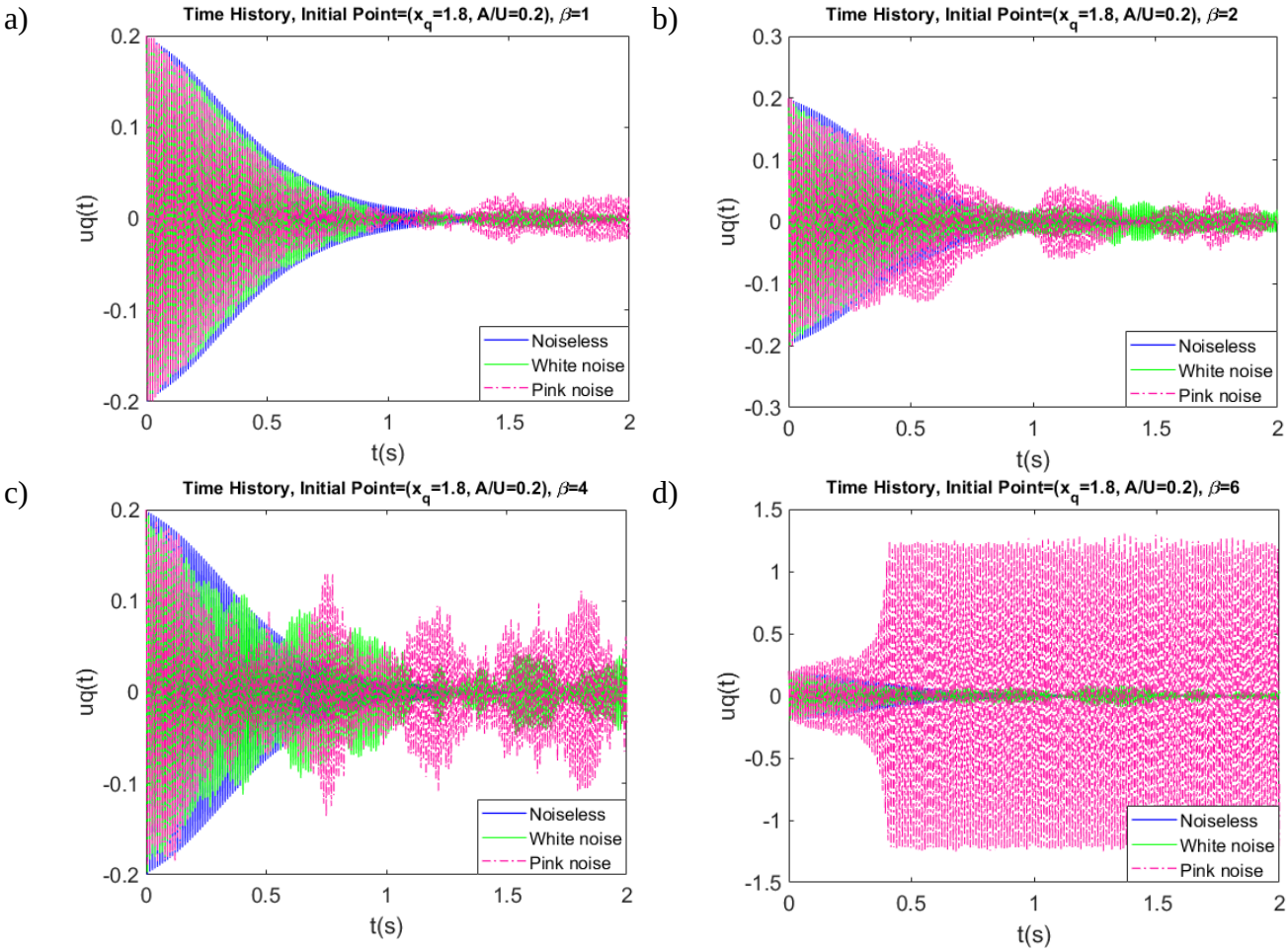

Figure 4: Time evolution of the acoustic field in a Rijke tube for a stable point in presence of white and pink noise a)Time histories for noiseless case, in presence of white noise and pink noise for $\beta = 1$ b) Time histories for noiseless case, in presence of white noise and pink noise for $\beta = 2$ c) Time histories for noiseless case, in presence of white noise and pink noise for $\beta = 4$ d) Time histories for noiseless case, in presence of white noise and pink noise for $\beta = 6$.

We now consider the unstable point ($x_q = 1.5, \frac{A}{U} = 0.01$), and investigate the effect of both types of noise. Figure 5 shows time history; its amplitude increases initially, and eventually a limit cycle is reached. In the absence of noise, the system behaves as shown by the blue curve. If noise is included, the limit cycle is reached faster. In other words, as we increase the noise intensity the transient time to a limit cycle will decrease; this effect is more pronounced for pink noise than for white noise.

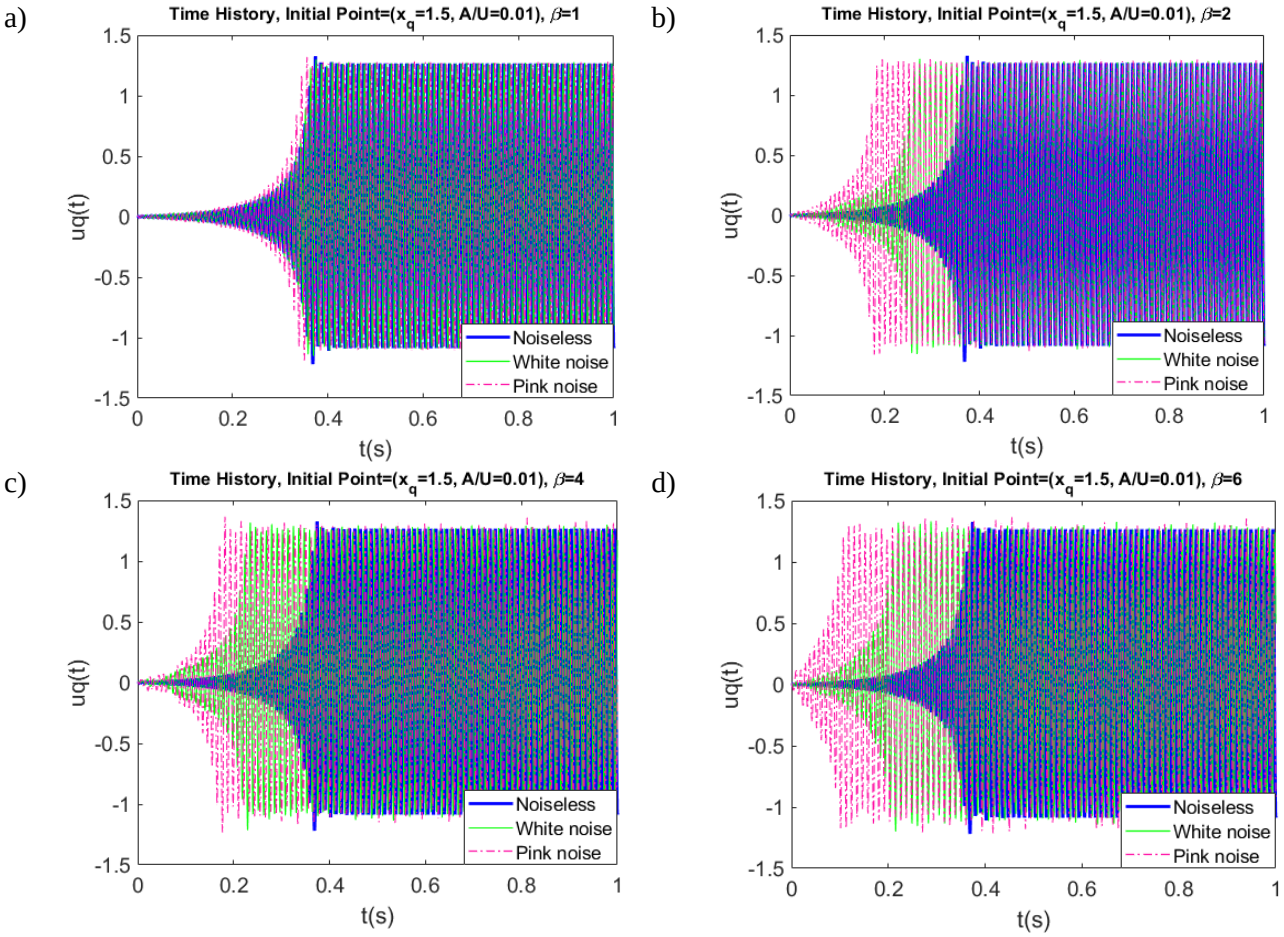

Figure 5: Time evolution of a Rijke tube for an unstable point in presence of white and pink noise Time histories for noiseless case, in presence of white noise and pink noise for $\beta = 1$ b) Time histories for noiseless case, in presence of white noise and pink noise for $\beta = 2$ c) Time histories for noiseless case, in presence of white noise and pink noise for $\beta = 4$ d) Time histories for noiseless case, in presence of white noise and pink noise for $\beta = 6$.

One of the nonlinear phenomena that occur in thermoacoustic systems are hysteresis effects. Bigongiari and Heckl [3], observed such behaviors in stability maps obtained by using a Green's function approach without noise. They varied a control parameter in the forward and backward direction and observed subcritical or supercritical Hopf bifurcations. We observed above that the presence of noise in thermoacoustic systems can trigger an instability and that the system becomes increasingly unstable as the strength of the noise increases. We therefore expect that noise will also affect the hysteresis zone by changing the subcritical Hopf bifurcation point.

In order to investigate the effect of noise on the hysteresis zone, we considered a quarter wave resonator ($R_0 = 1, R_L = -1$). We use the heater power K as bifurcation parameter, and start from an arbitrary valueK_1. In each step, we increased the heater power ($K_2 = K_1 + \Delta K$). At a certain value of K, we have an abrupt transition to high-amplitude oscillations. There is a subcritical Hopf bifurcation for our system at around K=1.1 (Figure 6, green curve). Then, we take the backward path and decrease the value of the heater power. In contrast to the forward path, we don't observe any sudden transition and the oscillation continues with a high amplitude (Figure 6, red curve). Hence, a hysteresis zone is observed. In the next step, we added noise and increased the noise intensity. As the

noise intensity increases, the system becomes unstable, and triggering occurs at a lower K value than without noise. In other words, the position of bifurcation point moves to the left when noise is present. This effect becomes more pronounced as the noise intensity increases. Consequently, the width of the hysteresis region decreases as we increase the noise level.

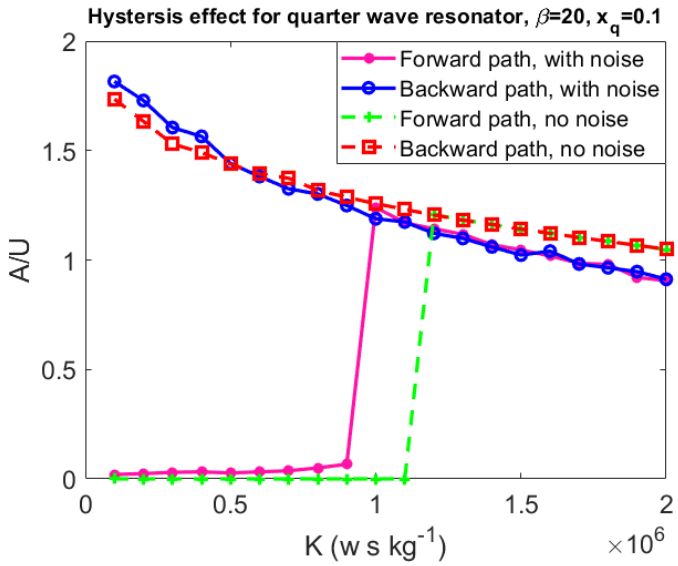

Figure 6: Hysteresis effect in presence of external noise for a quarter wave resonator, the heat source position is $x_q = 0.1$

6. Conclusion

In the present work, we performed an analytical investigation based on the Green's function approach to capture nonlinear dynamical phenomena in thermoacoustic systems in the presence of noise. One of the advantages of using a Green's function approach is its flexibility to apply in both time and frequency domains. Therefore, we obtain a time evolution (time-domain) and stability map (frequency domain) for a thermoacoustic system using our Green's function approach. We successfully validated these two different approaches.

In our study we extended our calculations by including external noise and compared the effects of pink noise and white noise. We found that pink noise has a stronger influence on the system. We considered a Rijke tube and showed that the transition time to reach the limit cycle decreases as the noise intensity increases. The transition time for pink noise is shorter than that for white noise with the same noise intensity. Moreover, we found that pink noise is more effective than white noise as trigger of a thermoacoustic instability. Furthermore, our study investigated the hysteresis effects in thermoacoustic systems with noise. To this end, we applied external noise to a quarter wave resonator and established that noise is an important parameter in that it decreases the width of the hysteresis region. This is because of triggering. Hence, increasing the noise level decreases the width of the bistable zone.

7. ACKNOWLEDGEMENTS

This work is part of the Marie Skłodowska-Curie Initial Training Network **Pol**lution **K**now-How and **A**batement (POLKA). We gratefully acknowledge the financial support from the European Commission under call H2020-MSCA-ITN-2018.

8. REFERENCES

[1] M. A. Heckl and M. S. Howe, "Stability analysis of the Rijke tube with a Green's function approach," *J. Sound Vib.*, vol. 305, no. 4–5, pp. 672–688, 2007.

[2] M. A. Heckl, "Analytical model of nonlinear thermo-acoustic effects in a matrix burner," *J. Sound Vib.*, vol. 332, no. 17, pp. 4021–4036, 2013.

[3] A. Bigongiari and M. A. Heckl, "A Green ' s function approach to the rapid prediction of thermoacoustic instabilities in combustors," pp. 970–996, 2016.

[4] G. Bonciolini, E. Boujo, and N. Noiray, "Output-only parameter identification of a colored-noise-driven Van-der-Pol oscillator: thermoacoustic instabilities as an example," *Phys. Rev. E*, vol. 95, no. 6, p. 62217, 2017.

[5] G. Bonciolini, E. Boujo, and N. Noiray, "Effects of turbulence-induced colored noise on thermoacoustic instabilities in combustion chambers," in *International Symposium: Thermoacoustic Instabilities in Gas Turbines and Rocket Engines*, 2016.

[6] V. Jegadeesan and R. I. Sujith, "Experimental investigation of noise induced triggering in thermoacoustic systems," *Proc. Combust. Inst.*, vol. 34, no. 2, pp. 3175–3183, 2013.

[7] I. C. Waugh and M. P. Juniper, "Triggering in a thermoacoustic system with stochastic noise," *Int. J. spray Combust. Dyn.*, vol. 3, no. 3, pp. 225–241, 2011.

[8] R. Rajaram and T. Lieuwen, "Acoustic radiation from turbulent premixed flames," *J. Fluid Mech.*, vol. 637, pp. 357–385, 2009.

[9] S. Arabi and M. Heckl, "A GREEN'S FUNCTION APPROACH TO STUDY THERMO-ACOUSTIC INSTABILITIES IN THE PRESENCE OF NOISE."